Revista Mexicana de Física **39**, *No. 4 (1993) 526–541*

Properties of the square-well fluid of variable width. V. Equation of state for intermediate ranges

ALEJANDRO GIL-VILLEGAS AND FERNANDO DEL RÍO*

Departamento de Física, Universidad Autónoma Metropolitana-Iztapalapa
Apartado postal 55-534, 09340 México, D.F., México

Recibido el 12 de enero de 1993; aceptado el 29 de abril de 1993

ABSTRACT. An equation of state (EOS), based on a perturbation expansion, is presented for the square-well (SW) fluid of intermediate ranges, $1.2 \leq \lambda \leq 1.75$, which are the most important for applications. This EOS complements previous theories for short and long ranges and is in very good agreement with computer simulation results for the SW internal energy and pressure for the ranges considered, for densities up to twice the critical and not too low temperatures. This equation compares favourably with other EOS from the literature. The vapor-liquid equilibrium predicted by the EOS agrees well with recent Gibbs ensemble MC calculations of Vega *et al.* except close to the critical point.

RESUMEN. Se presenta una ecuación de estado (EE) para el fluido de pozos cuadrados (PC), basado en un desarrollo perturbativo, para los alcances intermedios, $1.2 \leq \lambda \leq 1.75$, que son de interés en las aplicaciones. Esta EE complementa teorías previas para alcances cortos y largos, y concuerda bien con resultados simulados por computadora de la energía interna y la presión para los alcances considerados, y para densidades hasta el doble de la crítica y temperaturas no muy bajas. La EE propuesta se compara favorablemente con otras EE de la literatura. El equilibrio líquido-vapor predicho por la EE concuerda también con los recientes cálculos de Vega *et al.*, basados en el ensemble de Gibbs, excepto cerca del punto crítico.

PACS: 05.70.Ce; 64.10.+h

1. INTRODUCTION

During the last decade, the square-well (SW) fluid has played an important role as a model for thermodynamic [1–4] and transport [5–7] properties of classical fluids, and more recently, for adsorption and percolation phenomena [8,9]. The SW incorporates intermolecular repulsions and attractions in the simplest way, and is used as a reference in perturbation theory [10], and as a basis for theoretical equations of state of realistic simple fluids [11–13]. These applications require accurate equations for the thermodynamic properties of the SW system of variable width.

---

*Work performed while on sabbatical leave at the Departamento de Química Física, Universidad Complutense de Madrid, 28040, Madrid, Spain.

For two particles a distance r apart, the SW potential of diameter σ depth ϵ and range R is given by

$$u_{\mathrm{SW}}(r) = \begin{cases} \infty, & 0 < r < \sigma, \\ -\epsilon & \sigma < r < R, \\ 0, & R < r. \end{cases} \tag{1}$$

The thermodynamic properties of this system are quite well known from molecular dynamics (MD) and Monte Carlo (MC) simulations for various values of $\lambda = R/\sigma$ [14–20]. The vapour-liquid equilibrium, including the critical properties as a function of λ, has also been studied recently using the Gibbs ensemble MC technique [21]. The requirements of applications have induced the proposal of equations of state (EOS) for the SW fluid, which include EOS based on coordination number models [2,16,22–25] and on perturbation theory [1,4,26–28]. In spite of these extensive efforts, the predicted SW properties do not agree well with the simulated results away from its short ($\lambda \to 1$) and long ($\lambda \gg 1$) range limits.

This work reports and equation for the free energy of the SW fluid at the intermediate ranges ($1.2 \leq \lambda \leq 1.75$) which are relevant in applications [1,3,4,10,13]. Although the short- and long-range regions are theoretically interesting, the theories developed for these ranges fail for the practically important intermediate widths. A discussion of the accuracies obtained with the various approximations for long ranges has been presented recently [20]. The EOS obtained here improves the accuracy of the known SW EOS and agrees well with the simulation results for the SW pressure and internal energy [14–19] at intermediate ranges, $\rho^* = \rho\sigma^3 \leq 0.65$, and $T^* = kT/\epsilon \geq 0.8$, although it fails at higher densities and lower temperatures.

The high-temperature expansion of the SW free energy is analyzed in Sect. 2, and the main points needing improvement are identified and tackled in Sect. 3. The pressures and internal energies are compared in Sect. 3 with the MC and MD results [14–19]. Section 4 is devoted to a comparison with other EOS from the literature, and Sect. 5 discusses the SW thermodynamics as a function of λ, and its vapor-liquid equilibrium in comparison with Gibbs ensemble and MD results [21,29]. The conclusions are summarized in Sect. 6.

2. Analysis of the high temperature expansion

To write the EOS of the SW fluid of density $\rho = N/V$ and temperature T, we start from the high-temperature perturbation expansion (HTE) of the Helmholtz free energy A_{SW}, as introduced by Barker and Henderson [30]. If $a_{\mathrm{SW}} = A/NkT$ is the free energy per particle,

$$a_{\mathrm{SW}}(\eta, T^*) = a_{\mathrm{HS}}(\eta) + \frac{a_1(\eta,\lambda)}{T^*} + \frac{a_2(\eta,\lambda)}{T^{*2}} + a_{\mathrm{R}}(\eta, T^*, \lambda). \tag{2}$$

In this equation, $\eta = \pi\rho\sigma^3/6$ and $a_{\rm HS}$ is the hard-sphere (HS) free-energy, which will be taken from the Carnahan-Starling formula [31]. The SW mean-field term a_1 was obtained by Del Río and Lira for all ranges [28], and in the Percus-Yevick approximation by Flemming and Brugman [4]. For intermediate λ the mean-field approximation gives $a_{\rm SW}$ with an accuracy better than 1% only for $T^* \geq 20$, hence higher-order terms are needed [20]. Truncation of Eq. (2) after a_2 is quite accurate (with error below 10^{-3}) for $T^* > 5$ [20]. At small densities, a_2 is given by the Barker-Henderson local and macroscopic compressibility approximations (LCA, MCA) [30], and for $\lambda > 2$ by the Benavides-Del Río long-range approximation (LRA) [27]. The last term in (2) is the sum of all the higher-order contribution in the HTE

$$a_{\rm R}(\eta, T^*, \lambda) = \sum_{i=3}^{\infty} \frac{a_i(\eta, \lambda)}{T^{*i}}, \tag{3}$$

and will be called the remainder term. This term is necessary to predict adequately the SW vapor-liquid equilibrium for intermediate ranges. An expression for $a_{\rm R}$ can be obtained by using the LCA at all orders [32], but this result underestimates the free energy at moderate and high densities [33].

Therefore, in order to obtain an EOS for SW fluids of intermediate range, accurate at subcritical temperatures, it is necessary to improve the accuracy of the mean-field pressure derived from a_1 and of the known approximations (MCA, LCA and LRA) for a_2, and find an approximate expression for the remainder term $a_{\rm R}$.

3. EOS THE SQUARE-WELL FLUID

The mean-field term can be writte as [27,28]

$$a_1(\eta, \lambda) = \alpha_{13}(\eta)\lambda^3 + \alpha_{10}(\eta) + \alpha_{1\rm SR}(\eta, \lambda). \tag{4}$$

The van der Waals term $\alpha_{13} = -4\eta$, added to an exact $a_{\rm HS}$, gives the augmented VDW approximation (AVDW) which becomes exact in the Kac limit: $\epsilon \to 0$ and $\lambda \to \infty$, with $\epsilon\lambda^3 = \text{const.}$ [34,35]. The second term in Eq. (4) is the correction due to a finite range,

$$\alpha_{10}(\eta) = \tfrac{1}{2}[1 - K_{\rm HS}(\eta)], \tag{5}$$

where $K_{\rm HS} = kT(\partial\rho/\partial P_{\rm HS})_T$. The last or short-range term in (4) is

$$\alpha_{1\rm SR}(\eta, \lambda) = 12\eta \int_{\lambda}^{\infty} dx\, x^2 h_{\rm HS}(x), \tag{6}$$

and tends to zero when $\lambda \to \infty$. Interpolating a_1 between short and long ranges [26–28] gives $\alpha_{1\rm SR}$ for all λ withing 2% of the MC data [18], but error amplification makes the

pressure to deviate as much as 30%. In order to overcome this difficulty we propose a different interpolation form. Defining $b(\eta,\lambda)=\alpha_{1SR}(\eta,\lambda)/12\eta$, we let

$$b(\eta,\lambda)=\frac{\zeta e^{-\nu\xi}}{(1+\beta\xi)^n}\cos[\phi+\omega\xi(1+\gamma\xi)], \tag{7}$$

where $\xi=\lambda-1$, and $\zeta(\eta)$, $\nu(\eta)$, $\phi(\eta)$ are determined from the known short-range expansion (SRE), $\xi\to 0$ (see Appendix A). the parameters n, β and γ are chosen to optimize the shape of $b(\eta,\lambda)$ for $1.375<\lambda<1.75$ and $\rho^*\leq 0.6$. Their values are

$$n=0.860044,\quad \beta=5.487716,\quad \text{and}\quad \gamma=-0.415748.$$

When Eqs. (5) and (7) are used in (4), the mean-field compressibility factor $Z_1=\eta[\partial a_1/\partial\eta]$ has a r.m.s. deviation of 0.06 from the MC results [18,33,36] in $0.1\leq\rho^*\leq 0.8$, for $\lambda=1.375, 1.5, 1.625$ and 1.75.

For the term a_2 we start from the simple MCA which can be expressed as

$$a_{2MCA}=-\tfrac{1}{2}a_1(\eta,\lambda)K_{HS}(\eta), \tag{8}$$

and is obtained in closed form once a_1 is written as in (4). Nevertheless, for intermediate ranges, Eq. (8) is only good for $\rho^*\leq 0.2$. The LCA improves slightly the MCA, but at the cost of introducing in the pressure terms like $\partial^2 b(\eta,\lambda)/\partial\eta^2$, which amplify the error in $b(\eta,\lambda)$ itself. In this work we correct the MCA to reproduce the MC results and write

$$a_2=\frac{a_{2MCA}(\eta,\lambda)\Omega(\eta,\lambda)}{(1-\eta)^2}, \tag{9}$$

with

$$\Omega(\eta,\lambda)=1+\Omega_1(\lambda)\rho^*+\Omega_2(\lambda)\rho^{*2}+\Omega_3(\lambda)\rho^{*3}+\Omega_4(\lambda)\rho^{*4}, \tag{10}$$

where the coefficients Ω_i are given in Appendix B. The a_2 obtained from Eqs. (9) and (10) is within 1.4% of the MC results for $1.325\leq\lambda\leq 1.75$.

The high-order fluctuation terms in Eq. (3) tend to zero at high densities due to the HS repulsions. This fact is incorporated by the LRA [27], whose dominant term is proportional to K_{HS}^2. Hence, we propose a generalized MCA (GMCA) for the terms with $n\geq 3$:

$$a_n=a_n^0(\eta,\lambda,T^*)K_{HS}^2(\eta), \tag{11}$$

where a_n^0 incorporates the low density behavior of each term as obtained from the second and third SW virial coefficients [37] (see Appendix C). The GMCA in Eq. (11) for $n=3$ reproduces the MD results of Alder *et al.* for $\lambda=1.5$ within their uncertainty [14]. By Eq. (3), the remainder free-energy term takes the form

$$a_R(\eta,\lambda,T^*)=a_R^0(\eta,\lambda,T^*)K_{HS}^2(\eta), \tag{12}$$

where a_R^0 is the sum of all the a_n^0 for $n \geq 3$ adjusted to give the third virial coefficient at low temperatures (for details see Appendix C) [37], and is given by

$$a_R^0(\eta, \lambda, T^*) = -4\eta\left[(\lambda^3 - 1) - 1.5p(\lambda)\eta\right]W(T^*) + q(\lambda)t^3\eta^2, \tag{13}$$

where

$$p(\lambda) = \tfrac{211}{6} - 36\lambda^2 - 48\lambda^3 + 57\lambda^4 - \tfrac{49}{6}\lambda^6, \tag{14}$$

$$q(\lambda) = 746.5 - 1701.665\,\lambda + 1300\lambda^2 - 1000\lambda^3, \tag{15}$$

$$t = \exp\left(\frac{1}{T^*}\right) - 1, \tag{16}$$

and

$$W(T^*) = \exp\left(\frac{1}{T^*}\right) - 1 - \frac{1}{T^*} - \frac{0.5}{T^{*2}}. \tag{17}$$

The SW EOS for the Helmholtz free energy, referred to as EOS1, is obtained by substituting Eqs. (4), (9) and (12) in Eq. (2).

The internal energy of the SW fluid is given by

$$\frac{\beta U}{N} = \frac{3}{2} + \frac{u_1(\eta, \lambda)}{T^*} + \frac{u_2(\eta, \lambda)}{T^{*2}} + u_R(\eta, \lambda, T^*). \tag{18}$$

where $u_1 = a_1$, $u_2 = 2a_2$ and $u_R = -T^*[\partial a_R/\partial T^*]$. The SW internal energies predicted from EOS1 and (18) are in excellent agreement with the MC results [15,18]. In 45 states (with $0.4 \leq \rho^* \leq 0.8$; $0.8 \leq T^* \leq 4$; $\lambda = 1.375$, 1.5, 1.625 and 1.75) the r.m.s. deviation was 2.3%, only slightly larger than the estimated uncertainties in the simulations, although the deviation is larger at $\rho^* = 0.8$ and at the lower temperatures. Fig. 1 shows the behavior of $\Delta u_{SW} = \beta U/N - 3/2$ with λ at $T^* = 2$, for several ρ^*'s and the corresponding simulation data [15,17,18]. At not too high densities, $-\Delta u_{SW}$ grows with λ^3, as in the VDWA, but is more structured at higher densities.

The compressibility factor $Z = \beta P/\rho$ is

$$Z_{SW}(\eta, \lambda, T^*) = Z_{HS}(\eta) + \frac{Z_1(\eta, \lambda)}{T^*} + \frac{Z_2(\eta, \lambda)}{T^{*2}} + Z_R(\eta, \lambda, T^*), \tag{19}$$

where the notation explains the origin of each term. This EOS has the typical VDW form with the HS term making the positive contribution to the pressure. The mean-field term can be written as $Z_1 = Z_{1LR} + Z_{1SR}$, where Z_{1LR} arises from α_{13} and α_{10} and Z_{1SR} from α_{1SR}. For intermediate ρ^* and T^*, Z_{1LR} tends to cancel Z_{HS} and the contribution of Z_{1SR} becomes more important; this explains the difficulty in improving the attractive part of the classical VDW EOS after correcting the repulsive part Z_{HS}, as was done by Longuett-Higgins and Widom [38].

Figure 2 compares Z_{SW} at $\lambda = 1.5$, obtained from the EOS1 and Eq. (19), with MC results from the literature [15,16]. The pressures predicted by the EOS1 are in good

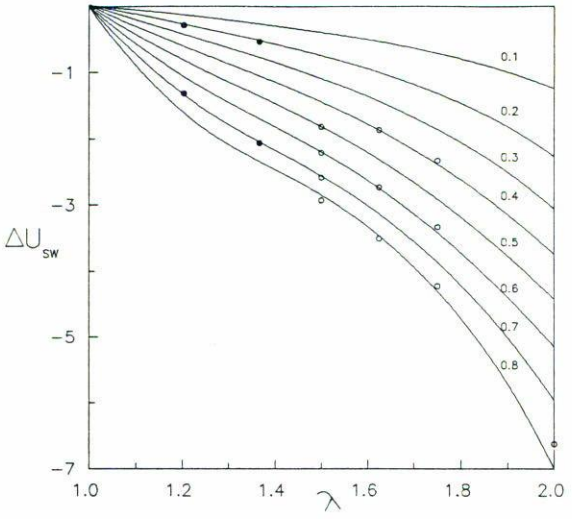

FIGURE 1. Excess internal energy of the SW fluid as a function of the range λ at $T^* = 2$ and various densities as labelled. The solid lines stand for the EOS1 in this work. Also shown are the MC results of Henderson *et al.* [15,18] (while circles) and of Rosenfeld and Thieberger [17] (black circles).

agreement with the simulation results for $T^* \geq 0.8$ and $\rho^* \leq 0.65$. The deviation in Z_{sw} between theory and simulations at $\rho^* \geq 0.7$, is more marked than for U. The comparison with the MC results at other ranges is similar. Typical SW pressure isochores are shown in Fig. 3, where the EOS1 is compared with recent MD results by De Lonngi *et al.* [19] for $\lambda = 1.4$. The agreement is excellent and similarly for $\lambda = 1.6$.

4. COMPARISON WITH OTHER EOS

A detailed comparison has been made between EOS1 and other SW EOS from the literature. Among the SW EOS based on a perturbation expansion there are three first-order EOS: The original VDW equation, the augmented VDW equation (AVDW) which used an accurate a_{HS}, and the mean-field EOS of del Río and Lira (DRL) [28]. Four second-order EOS differ in various approximations for a_{HS}, a_1 and a_2, and are those of Ponce & Renon (PR) [39], Aim & Nezbeda (AN) [1], Flemming & Brugman (FB) [4], and the long-range Benavides-Del Río equation (BDR) [20,27].

Several authors have proposed SW EOS based on coordination numbers [40]: 1) The two equations of Lee, Lombardo and Sandler (LLS1 & LLS2, given respectively in Eqs. (15) and (21) of Ref. [2]) and the more recent Lee-Sandler equation (LS) [22]; 2) the Lee-Chao equation (LCh) [24]; and 3) the two equations of Guo, Wang and Lu (GWL1 & GWL2, Eqs. (21) and (22) of Ref. [16], respectively). The last EOS considered is that of Song and Mason (SM) [41], which, although originally proposed for continuous potentials, provides a simple closed-form formula for the SW fluid.

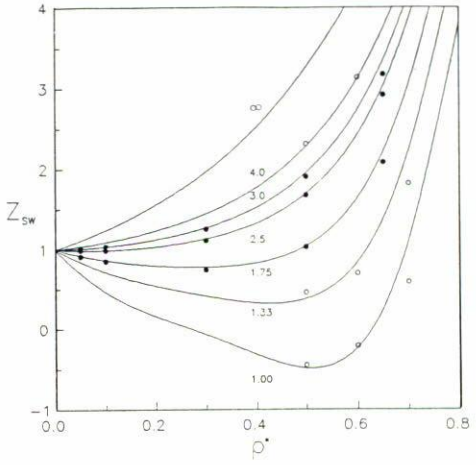

FIGURE 2. Compressibility factor Z_{sw} of the $\lambda = 1.5$ SW fluid along several isotherms as labelled. The solid lines and white circles have the same meaning as in Fig. 3. The black circles stand for the MC results of Guo *et al.* [16].

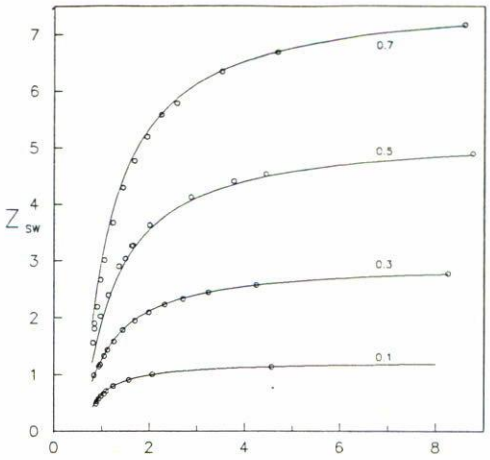

FIGURE 3. Compressibility factor Z_{sw} of the $\lambda = 1.4$ SW fluid along selected isochores as labelled. Shown are EOS1 (full line) and the MD results of De Lonngi *et al.* (circles) [19].

The EOS developed in this paper and the 14 EOS from the literature were tested against the simulation results available. These include results of MC [15–18] and MD [14,19] simulations. Two-phase states were eliminated using the vapor-liquid coexistence line by Vega *et al.* [21] to obtain a total of 118 MC states and 273 MD states. Restricted sets of states were obtained by eliminating densities $\rho^* \geq 0.7$, temperatures $T^* < 0.8$ and the extreme ranges $\lambda = 1.125$ and 2.00; these restricted MC and MD sets comprised 63 and 186 states respectively.

The r.m.s. deviations in the compressibility factor Z_{sw} of the 15 EOS from the sets of simulation results are shown in Table I: from the complete wide sets (columns 2 and 3) and restricted sets (columns 4 and 5). Deviations are smaller from the MD sets than

TABLE I. Test of the SW EOs against simulated results. Shown are the r.m.s. deviations in the compressibility factor Z. The columns correspond to the wide (a) and restricted (b) sets of states for Monte Carlo (MC) and molecular dynamics (MD) data.

EOS	MC (a)	MD (a)	MC (b)	MD (b)
No. of states	118	273	63	186
VDW	14.849	18.820	18.729	21.786
AVDW	0.784	0.631	0.236	0.142
DRL	0.798	0.415	0.284	0.185
PR	0.910	0.487	0.345	0.263
AN	0.823	0.546	0.302	0.225
FB	1.151	0.151	0.173	0.065
BDR	0.820	0.533	0.227	0.149
SM	1.452	1.922	0.381	0.219
LCh	1.594	1.134	0.630	0.237
LS	1.090	0.412	0.583	0.292
GWL1	1.561	0.874	0.629	0.451
GWL2	1.699	1.103	0.570	0.203
LLS1	1.185	0.541	0.584	0.362
LLS2	1.649	0.640	0.670	0.175
EOS1	0.720	0.341	0.113	0.054

from the MC sets, perhaps because the MD simulations cover a narrower set of ranges ($1.4 \leq \lambda \leq 1.6$). Except for VDW, which fares equally badly for both sets, all other EOS are much better for the restricted than for the wider sets. In general, the PT equations are more accurate than the coordination number models. The latter, besides being simpler, have been developed mostly for $\lambda = 1.5$ and are closer to the PT EOS for the restricted MD set. It is somewhat discouraging that over the wide MC set, which includes λ's outside the intermediate range region, only one equation (EOS1) is better than AVDW. In the three remaining sets (wide MD and restricted MC and MD, which are in the intermediate range region) the two best equations are EOS1 and FB.

A good EOS should be able to predict correctly the virial coefficients. The second virial coefficient B_2 predicted by the SW EOS1 is exact, but not so for the BF EOS. The third virial coefficient obtained from EOS1 is very close to the exact Kihara formula [37] as shown in Fig. 4, which also includes the values derived from the GWL2 EOS (which gives the best B_3 among the coordination number models considered by Guo *et al.* [16]).

5. THERMODYNAMIC BEHAVIOR AND VAPOR-LIQUID EQUILIBRIUM

The EOS1 gives the behavior of the SW properties with λ, *i.e.*, with a change in the *shape* of the potential. Figure 5 shows the free energy $\Delta a_{\mathrm{SW}} = a_{\mathrm{SW}} - a_{\mathrm{id}}$ for $T^* = 2$ and several densities. The values of Δa_{SW} at $\lambda = 1$ should equal $\Delta a_{\mathrm{HS}} = -\Delta s_{\mathrm{HS}}$. The SW excess entropy $\Delta s_{\mathrm{SW}} \simeq \Delta s_{\mathrm{HS}}$ because the mean-field term does not contribute. When λ

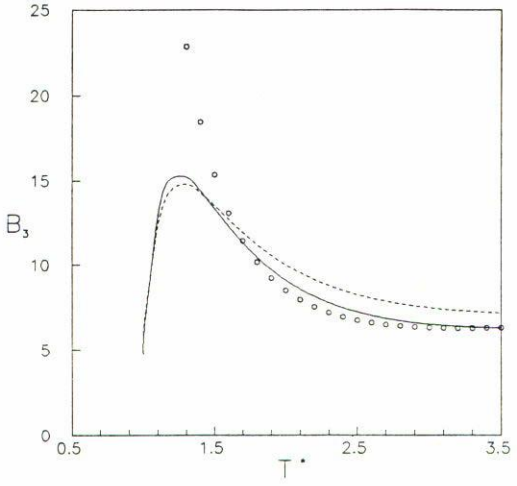

FIGURE 4. Third virial coefficient of the $\lambda = 1.5$ SW as obtained from Kihara's exact expression [37] (solid line); EOS1 (dashed line), and GWL2 EOS [16] (circles).

increases, $\Delta a_{\rm SW} \propto \lambda^3$ due to $\Delta u_{\rm SW}$. Due to the combined effects of $\Delta s_{\rm SW}$ and $\Delta u_{\rm SW}$, $\Delta a_{\rm SW}$ increases with ρ^* for $\lambda < 1.4$, whereas for $\lambda > 1.8 \Delta a_{\rm SW}$ decreases with ρ^*; for intermediate ranges, $\Delta a_{\rm SW}$ goes through a minimum in ρ^*. The derivative of $\Delta a_{\rm SW}$ with λ is proportional to $y(\lambda)$ [28], the background correlation function at $x = \lambda$, and the attractive force is also proportional to $y(\lambda)$. Hence, from Fig. 5, the attractive force will be monotonic with λ (the VDWA predicts $y(\lambda) = 1$) at small densities or long ranges, but will go through a minimum and a maximum for high densities.

The behavior of $Z_{\rm SW}(\lambda)$ is shown in Fig. 6 for $T^* = 2$ and several densities, together with the corresponding simulation results [15,17–19]. In general $Z_{\rm SW}$ decreases with increasing λ as in the VDW model, but at higher densities there is a loop in $Z_{\rm SW}(\lambda)$, also present in the simulation results, which is due to the oscillations in $y(\lambda)$. This loop cannot be derived from the VDWA and is produced by the short-range term $a_{\rm 1SR}$.

Figure 7 shows the orthobaric densities for $\lambda = 1.5$ as obtained from EOS1, as well as the AVDW orthobaric curves, and the Gibbs ensemble MC (GEMC) and MD simulation results [21,29]. The behavior shown is similar for other ranges. The orthobaric densities obtained with the EOS1 are in good agreement with the simulation data, except close to the critical point. The prediction of the EOS agrees well with the MD simulations down to $T^* = 0.8$, which is the lower confidence limit of this EOS.

Figures 8 and 9 show the behavior of $T_{\rm c}$ and $\rho_{\rm c}$ with λ as obtained from the EOS1 and from the AVDW approximation. These are compared with second-order perturbation theory (PT2) results by Henderson *et al.* [15,18] and with the GEMC results [21], (at $\lambda = 1.5$ one also has the MD values by Alder *et al.* [14]). Being effectively a two- parameter EOS, the AVDW approximation predicts $\rho_{\rm c} = 0.25$ and $Z_{\rm c} = 0.36$ for all λ, whereas $T_{\rm c}^*$ (and also $P_{\rm c}^*$) grows with λ^3 as in Fig. 8. At $\lambda = 3$, the AVDW model is essentially

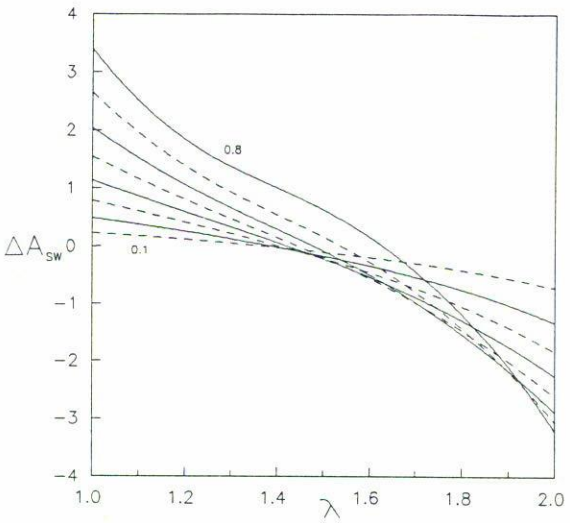

FIGURE 5. Excess Helmholtz free energy for the SW fluid as a function of the range λ according to the EOS1 of this work. The curves correspond to reduced densities from 0.1 to 0.8 and the temperature is $T^* = 2.0$.

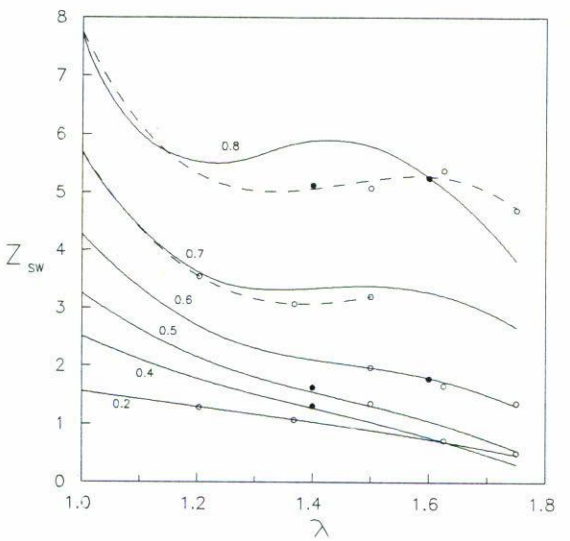

FIGURE 6. Compressibility factor of the SW fluid as a function of the range λ at $T^* = 2$ according to EOS1 of this work (full lines) for the densities as labelled. Also shown are the MC results of Henderson *et al.* [15,10] and Rosenfeld and Thieberger [17] (white circles), and the MD results of De Lonngi *et al.* [19], (black circles). The dashed lines are polynomial interpolations of the simulation results.

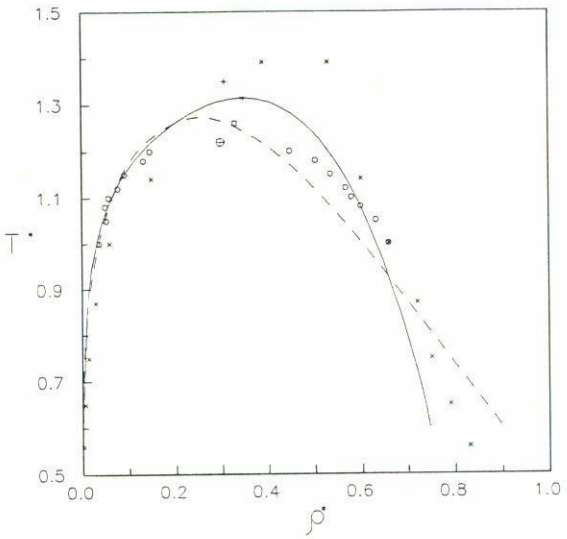

FIGURE 7. Vapor-liquid equilibrium of the SW with $\lambda = 1.5$. Orthobaric line from EOS1 (full line), AVDW approximation (dashed line), GEMC results of Vega *et al.* [21] (circles), MD results of Chapela *et al.* [29] (×). The position of the critical point is: EOS1 (*), second-order perturbation theory [18] (+), Gibbs ensemble [21] (+), and MD result of Alder *et al.* [14] ( ).

exact [20]. For lower λ's, the AVDW prediction of ρ_c is far away from the GEMC results, but that of T_c^* is surprisingly close to them.

The critical density increases over the AVDW value when $\lambda < 2$, see Fig. 9, and this tendency is picked up, although overestimated, by the EOS1. This overestimation for $\lambda < 1.4$, together with a slightly higher T_c^*, makes P_c^* higher than in the GEMC results.

6. CONCLUSIONS

The EOS1 is the most accurate among the SW EOS available from the literature when tested against published simulation data, in the fluid states $\rho^* \leq 0.65$ and $T^* \geq 0.8$, and for the intermediate ranges $1.2 \leq \lambda \leq 1.75$, except for a small region around the critical point. The other EOS of comparable accuracy is the equation of Flemming and Brugman [4]. These EOS are based on perturbation theory and are rather more complicated than the simpler, although less accurate, EOS based on coordination number models.

Together with the SW EOS previously proposed for short and long ranges [26,27], the EOS1 provides quite accurate knowledge about the dependence of the SW thermodynamic properties, including the vapor-liquid equilibrium, on the width of the potential well, all the way from very narrow to very wide potential wells where the AVDW approximation becomes exact. The SW properties in the intermediate range region are the result of the balance among several terms in the EOS, which are rather difficult to model, particularly at high densities and close to the critical point. This work shows that the most important term needing improvement is the short-range term α_{1SR} of the mean-field free energy.

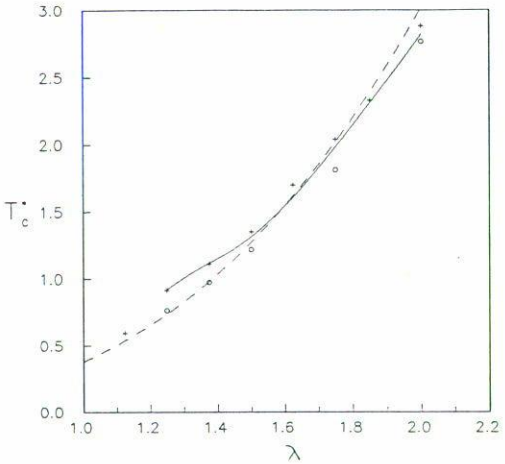

FIGURE 8. Reduced critical temperature T_c^* of the SW fluid as a function of the range λ. The symbols have the same meaning as in Fig. 7.

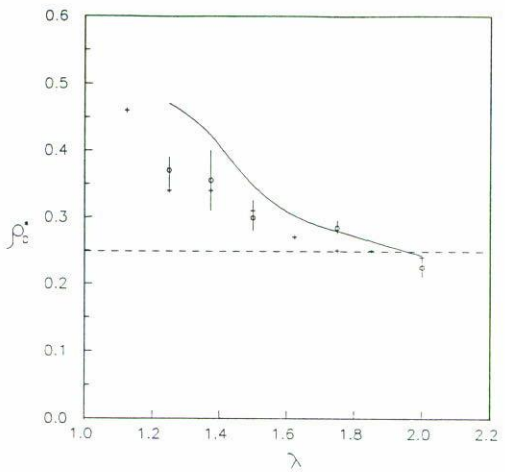

FIGURE 9. Reduced critical density ρ_c of the SW fluid as a function of the range λ. The symbols have the same meaning as in Fig. 8. The vertical lines show the error bars of the Gibbs ensemble calculation [21].

The SW EOS here proposed can be used to generate EOS of more realistic fluids, *i.e.*, with continuous potentials, an application that will be presented by the authors in a future communication.

ACKNOWLEDGEMENTS

This work was partially supported by the Dirección General de Investigación Científica y Técnica (Spain), and the Consejo Nacional de Ciencia y Tecnología (México). AGV wishes to thank the Departamento de Química Física of the Universidad Complutense de Madrid for its hospitality and the partial support of the Rotary Club of Iztapalapa,

México. The authors express their gratitute to G. Jackson, I.A. McLure, and L.F. Rull for facilitating their Gibbs ensemble SW simulation results prior to publication.

APPENDIX A

The short-range expansion of $b(\eta, \lambda)$ reads

$$b(\eta, \lambda) = \sum b(\eta)(\lambda - 1)^m, \tag{A1}$$

where $b_m(\eta) = \partial^m b(\eta, \lambda)/\partial\lambda^m$ evaluated at $\lambda = 1$. Defining $b_1^* = b_1/b_0$, the desired functions in Eq. (7) are obtained from (A1) as

$$\nu = \mu - n\beta, \tag{A2}$$

$$\omega^2 = \left[n\beta^2 - 2b_2^* + 2\gamma b_1^* - 2\mu(b_1^* - \gamma) - \mu^2\right], \tag{A3}$$

$$\tan\phi = -\frac{b_1^* + \mu}{\omega}, \tag{A4}$$

$$\zeta = \frac{b_0}{\cos\phi}, \tag{A5}$$

and where μ is the solution of

$$2\gamma\mu^2 + \left[-6\gamma^2 + 4\gamma b_1^* + b_1^{*2} - 2b_2^* + n\beta^2\right]\mu + \left[-6\gamma^2 b_1^* + (6b_2^* - 3n\beta^2 - b_1^{*2})\gamma + (b_1^* - \beta)n\beta^2 + b_1^* b_2^* - 3b_3^*\right] = 0 \tag{A6}$$

From the previous work of Del Río and Lira [28], it is known that

$$b_0 = \frac{1}{3} + \frac{K_{\mathrm{HS}} - 1}{24\eta}, \tag{A7}$$

$$b_1 = 1 - y_{\mathrm{HS}}^0, \tag{A8}$$

$$b_2 = b_1 - \frac{1}{2}\frac{\partial y_{\mathrm{HS}}^0}{\partial x}, \tag{A9}$$

$$b_3 = \frac{b_1}{3} - \frac{2}{3}\frac{\partial y_{\mathrm{HS}}^0}{\partial x} - \frac{1}{6}\frac{\partial^2 y_{\mathrm{HS}}^0}{\partial x^2}, \tag{A10}$$

where $x = r/\sigma$, y_{HS}^0 is the contact value of the HS cavity function, obtained from the CS EOS, and its first and second x-derivatives are known functions of the density [26].

APPENDIX B

The polynomials $\Omega_n(\lambda)$ of Eq. (10) for the SW EOS1 are

$$\Omega_1(\lambda) = -150.4141 + 295.5278\,\lambda - 188.7726\,\lambda^2 + 39.05170\,\lambda^3,$$

$$\Omega_2(\lambda) = 651.0186 - 1182.422\,\lambda + 701.2853\lambda^2 - 135.4891\,\lambda^3,$$

$$\Omega_3(\lambda) = -86.89659 - 15.0961\,\lambda + 127.1438\,\lambda^2 - 51.78439\,\lambda^3,$$

$$\Omega_4(\lambda) = -775.5074 + 1603.865\,\lambda - 1089.664\,\lambda^2 + 243.7498\,\lambda^3.$$

APPENDIX C

At low densities, the SW pressure is given by the virial expansion

$$\frac{\beta P}{\rho} = 1 + B_2(T^*, \lambda)\eta + B_3(T^*, \lambda)\eta^2 + \cdots, \tag{C1}$$

whose coefficients B_L are functions of T^* and λ. The first two are

$$B_2(T^*, \lambda) = 4\big[1 - (\lambda^3 - 1)t\big], \tag{C2}$$

and, for $\lambda < 2$ [37],

$$B_3(T^*, \lambda) = 10 + I_1(\lambda)t + I_2(\lambda)t^2 + I_3(\lambda)t^3, \tag{C3}$$

where $t = \exp(1/T^*) - 1$, and I_1, I_2, I_3 are polynomials in λ with different coefficients for $\lambda < 2$ and $\lambda > 2$. Expanding the exponential in t in powers of the inverse temperature $1/T^*$, the SW virial series $(C1)$ can be used to find the low density expansion of the terms a_n. One finds that the for a_1 and a_2 in Eqs. (4) and (9), give the correct contribution to B_2 but not to B_3. In the last case, the discrepancy comes from the densities derivative of $b(\eta, \lambda)$ and the factor $\Omega(\eta, \lambda)$ used to correct the MCA in a_2.

The third-order term a_3 must be, when $\eta \to 0$,

$$a_3^0(\eta, \lambda) = -\tfrac{2}{3}(\lambda^3 - 1)\eta + p(\lambda)\eta^2 + \cdots \tag{C4}$$

where $p(\lambda)$ is the polynomial of equation (14), for $\lambda \leq 2$.

For the next terms a_n^0 one obtains equations similar to $(C4)$ and (14). The contribution proportional to η in a_n^0 is $-4(\lambda^3 - 1)/n!$, but it is not possible to express in a similar condensed formula the term proportional to η^2, because to each a_n^0 corresponds a different sixth-degree polynomial in λ. However, an analysis of a_n^0 for $n = 3, 4$ and 5 shows that they have very similar behavior for supercritical temperatures, which we will assume to hold for all orders. Hence the a_n^0 will be approximated by

$$a_n^0(\eta, \lambda) = -\frac{\eta\big[4(\lambda^3 - 1) + 6p(\lambda)\eta\big]}{n!} \qquad (n \geq 3), \tag{C5}$$

where the exact contribution to the second virial coefficient ($C2$) is already included. By ($C5$), the low-density remainder term in (3) can now be expressed in closed form

$$a_R^0(\eta, \lambda, T^*) = -4\eta\left[(\lambda^3 - 1) - 1.5\, p(\lambda)\eta\right] W(T^*). \qquad (C6)$$

where $W(T^*) = \exp(1/T^*) - 1 - 1/T^* - 0.5/T^{*2}$. At subcritical temperatures, where the approximation (C5) falls, Eq. (6) is corrected by introducing a term proportional to t^3. This term determines the low temperature behavior of B_3 and does not contribute with terms proportional to $1/T^*$ or $1/T^{*2}$, which are already considered in a_1^0 and a_2^0. The final expression for a_R^0 is Eq. (13), where $q(\lambda)$, Eq. (15), was obtained by adjusting the values of the third virial coefficient, calculated from the SW EOS1, with the exact Kihara result (RC3R), in the λ interval considered in this work.

REFERENCES

1. I. Nezbeda, and K. Alm, *Fluid Phase Equil.* **17** (1984) 1.
2. K.H. Lee, M. Lombardo and S.I. Sandler, *Fluid Phase Equil.* **21** (1985) 177.
3. E. Fernández-Fassnacht, and F. del Río, *Rev. Mex. Fís.* **33** (1987) 200.
4. P.D. Flemming III, and R.J. Brugman, *AIChE Journal* **33** (1987) 729.
5. A.F. Collings, and I.L. McLaughin, *J. Chem. Phys.* **73** (1980) 3390.
6. C.G. Joslin, C.J. Gray, J.P.C. Michels and J. Karkheck, *Molec. Phys.* **69** (1990) 535.
7. P.A. Monson, *Molec. Phys.* **70** (1990) 401.
8. F. del Río and A. Gil-Villegas, *J. Phys. Chem.* **95** (1991) 787.
9. Y.C. Chiew, and Y.N. Wang, *J. Chem. Phys.* **89** (1988) 6385.
10. D.A. de Lonngi, F. del Río, *Molec. Phys.* **48** (1983) 293; *Molec. Phys.* **56** (1985), 691.
11. F. del Río and A. Gil-Villegas, *Molec. Phys.* **76** (1992) 21-28.
12. F. del Río and A. Gil-Villegas, *Molec. Phys.* **77** (1991) 223.
13. A. Gil-Villegas, M. Chávez and F. del Río, *submitted to Rev. Mex. Fís.* (1992).
14. B.J. Alder, D.A. Young, and M.A. Mark, *J. Chem. Phys.* **56** (1972) 3013.
15. D. Henderson, W.G. Madden, and D.D. Fitts, *J. Chem. Phys.* **64** (1976) 5026.
16. M.X. Guo, W.C. Wang, and H.Z. L, *Fluid Phase Equil.* **60** (1990) 221.
17. Y. Rosenfeld, and R. Thieberger, *J. Chem. Phys.* **63** (1975) 1875.
18. D. Henderson, O.H. Scalise, and W.R. Smith, *J. Chem. Phys.* **72** (1980) 2431.
19. D.A. de Lonngi, P.A. Lonngi and J. Alejandre, *Molec. Phys.* **71** (1990) 427.
20. A.L. Benavides, J. Alejandre and F. del Río, *Molec. Phys.* **74** (1991) 321.
21. L. Vega, E. de Miguel, L.F. Rull, I.A. McLure and G. Jackson, *J. Chem. Phys.* **96** (1992) 2296.
22. K.H. Lee, and S.T. Sandler, *Fluid Phase Equil* **34** (1987) 113.
23. K.H. Lee, I.R. Dodd and S.T. Sandler, *Fluid Phase Equil.* **50** (1989) 53.
24. R.J. Lee, and K.C. Chao, *Molec. Phys.* **61** (1987) 1431.
25. M.X. Guo, W.C. Wang, and H.Z. Lu, *Fluid Phase Equil.* **60** (1990) 37.
26. F. del Río and L. Lira, *Molec. Phys.* **61** (1987) 275.
27. A.L. Benavides, and F. del Río, *Molec. Phys.* **68** (1989(983.
28. F. del Río and L. Lira, *J. Chem. Phys.* **87** (1987) 7179.
29. G. Chapela, S. Martínez-Casas, and C. Varea, *Chem. Phys.* **86** (1987) 5683.
30. J.A. Barker and D. Henderson, *J. Chem. Phys.* **47** (1967) 2856; *Ibid* **47** (1967) 4714.
31. N.F. Carnahan and K.E. Starling, *J. Chem. Phys.* **51** (1969) 635.
32. E. Praestgaard and S. Toxvaerd, *J. Chem. Phys.* **53** (1970) 2389.
33. J.A. Barker and D. Henderson, *Rev. Mod. Phys.* **48** (1976) 587.

34. M. Kac, G.E. Uhlenbeck and P.C., Hammer, *J. Math. Phys.* **4** (1963) 216; *Ibid* **4** (1963) 2239; *Ibid* **5** (1964) 60.
35. O. Penrose and J.L. Lebowitz, *J. Math. Phys.* **13** (1972) 604.
36. D. Henderson, *private communication.*
37. T. Kihara, *Nippon-Sugaku-Buturigakukaisi,* **17** (1943) 11.
38. H.C. Longuett-Higgins and B. Widom, *Molec. Phys.* **8** (1964) 549.
39. L. Ponce and H. Renon, *J. Chem. Phys.* **64** (1976) 638.
40. S.I. Sandler, *Chem. Eng. Ed.* **24** (1990) 12.
41. Y. Song and E.A. Mason, *J. Chem. Phys.* **91** (1989) 7840.